JOURNAL OF MATERIALS SCIENCE 23 (1988) 3721–3731

Annealing study of poly(etheretherketone)

PEGGY CEBE
Applied Sciences and Microgravity, Experiments Section, Jet Propulsion Laboratory, California Institute of Technology, Pasadena, California 91109, USA

Annealing of poly(etheretherketone), PEEK, has been studied for two materials cold crystallized from the rubbery amorphous state. The first material is a low molecular weight PEEK synthesized in our laboratory; the second is commercially available neat resin. Differential scanning calorimetry was used to monitor the melting behaviour of annealed samples. The effect of thermal history on melting behaviour is very complex and depends upon annealing temperature, residence time at the annealing temperature, and subsequent scanning rate. Thermal stability of both materials is improved by annealing, and for an annealing temperature near the melting point, the polymer can be stabilized against reorganization during the scan. Variations of density, degree of crystallinity, and X-ray long period were studied as a function of annealing temperature for the commercial material. Wide angle X-ray scattering was used to study the structure of annealed PEEK. An additional scattering peak was observed at higher *d*-spacing when annealed samples were cooled quickly.

1. Introduction

The effects of annealing on microstructure and mechanical properties have been studied recently for a variety of semicrystalline thermoplastic polymers, including polypropylene [1, 2], poly(ethylene terephthalate) [3], and polycarbonate [4, 5]. Properties such as impact strength, shear band morphology, craze ductility, and fracture have been related to the morphological changes caused by annealing treatments. In poly(etheretherketone), PEEK, a newly developed high-performance thermoplastic, changes in mechanical properties have been observed after annealing of cold crystallized material [6], and after zone-annealing of drawn material [7]. The current study was undertaken to determine the effects of various annealing treatments on the microstructure and properties of PEEK.

Currently, PEEK is being used as composite matrix material in applications requiring thermal stability, resistance to solvent attack, and/or resistance to damage by irradiation. The morphology [8–12], structure [8, 13–15], and crystallization and melting [16–21] of PEEK have been reported. Because of its low ultimate degree of crystallinity, PEEK can be quenched from the melt into the glassy amorphous state, and crystallized by heating above the glass transition temperature. Crystallization from a state of low chain mobility generally results in a very imperfect crystal structure. Consequently, cold crystallization of the amorphous polymer may result in a material that will undergo significant property changes when the temperature is increased. Annealing treatments after crystallization can be utilized to improve the thermal stability of cold crystalized material. This perfection of crystal structure may come about through fold surface smoothing, lamellar thickening, or removal of defect regions in the crystal. It is of fundamental importance to determine the effect of annealing treatments on the polymer structure and properties so that the effect on bulk mechanical properties can be understood. The subject of the current study was the influence of annealing on physical properties such as melting behaviour, crystallinity and crystal perfection, and X-ray long period. We have used the techniques of differential scanning calorimetry and wide- and small-angle X-ray scattering to study these effects in two PEEK materials of different molecular weights.

2. Experimental section

2.1. Starting materials

Two PEEK materials were used for this study: low molecular weight PEEK synthesized in our laboratory according to the method of Attwood *et al.* [22], and commercially available pellet grade resin (ICI Americas, Inc.). We will refer to these materials as LMW-PEEK and C-PEEK, respectively. Results of elemental analysis are listed in Table I. Relative viscosity and end-group analysis was used to establish the relative molecular weights of LMW-PEEK and C-PEEK. The relative viscosity of LMW-PEEK was 1.3 (25° C, 98% H_2SO_4 at 1 g/100 ml concentration) compared to 2.4 for C-PEEK.

We can make a rough estimate of the molecular weight of LMW-PEEK from the conditions of the synthesis. (Other methods of molecular weight determination use light scattering or gel permeation chromatography [22].) LMW-PEEK was synthesized from (F–ϕ–CO–ϕ–F) + (KO–ϕ–OK) where the initial mole ratio of the fluorine containing component to the potassium containing unit was 1.102. The maximum number average molecular weight was estimated to be 5900, calculated by assuming an extent of reaction $p = 1$ [24].

The minimum number average molecular weight

0022–2461/88 $03.00 + .12

TABLE I Elemental analysis (%) of poly(etheretherketones) used in annealing study

Element	LMW-PEEK*	LMW-PEEK†	C-PEEK
Carbon	78.78	76.90	79.17
Hydrogen	4.21	4.21	4.26
Potassium	0.19	< 0.04	< 0.02
Fluorine	0.99	0.79	0.17
Sulphur	0.10	0.71	0.11

*LMW-PEEK as-synthesized.
†LMW-PEEK precipitated from H_2SO_4.

of LMW-PEEK was estimated from the results of elemental analysis. The first column in Table I lists the per cent composition for as-prepared LMW-PEEK. As fluorine terminates both chain ends, the large amount of potassium, 0.19%, arises from formation of KF, a by-product of the synthesis. To remove excess KF, the LMW-PEEK was disolved in H_2SO_4, precipitated, and washed. The second column in Table II shows the composition of this material. Chains become sulphonated in H_2SO_4 as seen by the high sulphur content, but the amount of KF has been significantly reduced. The percentage of fluorine at the chain ends is 80% in the as-prepared material, and at least 76% in the H_2SO_4-treated material. The minimum number average molecular weight of LMW-PEEK thus lies between 4750 and 5000. The actual extent of reaction was estimated to be $p = 0.99$.

Conditions of synthesis are not known for the C-PEEK material. However, the number of moles of potassium is small compared to fluorine, so fluorine is assumed to terminate both chain ends in C-PEEK. This results in an estimated number average molecular weight of 22 400 for C-PEEK, or about 4.5 times that of LMW-PEEK.

2.2. Sample treatment and characterization

To prepare samples for the annealing studies, C-PEEK pellets were compression molded between ferrotype plates at 400° C. The resultant thin films were quenched to form amorphous material. The as-prepared LMW-PEEK was used in the annealing experiments. The LMW-powder degraded at 370° C, and a lower temperature of 350° C was used for this material. The powder was simply placed between ferrotype plates in a Mettler FP80 hot stage and gently pressed to form irregularly shaped thicker samples. After 10 min residence time at 350° C, the LMW-PEEK was quenched.

For long-time annealing, samples were installed into an air flow oven preset at the annealing temperature. One set (described in Section 3.1) was first crystallized at 176° C for 24 h, then heated directly to the annealing temperature and held an additional 24 h. Another set of films (described in Section 3.2) was heated to the annealing temperature and held for 24 h. In both cases, it took about 30 min for the sample temperature to equilibrate after insertion into the oven or after the temperature was changed. Samples were cooled quickly after treatment.

A DuPont 1090 Thermal Analyser was used to provide rapid heating rates for studies of short-time annealing (described in Section 3.3). Small samples of the amorphous films were rapidly heated from room temperature to the annealing temperature, then quenched and subsequently scanned at 20° C min^{-1}. The samples reached the annealing temperature in under 3 min.

Degree of crystallinity for C-PEEK was determined using density and differential scanning calorimetry (DSC). The densities of the amorphous and crystalline materials were assumed to be 1.264 and 1.378 g cm^{-3}, respectively [12]. The heat of fusion of perfectly crystalline C-PEEK was assumed to be 130 J g^{-1} [8]. LMW-PEEK could be investigated using WAXS and DSC, but the sample surfaces containg many irregularities which precluded accurate density measurements.

A Siemens D-500 diffractometer with nickel filtered Cu$K\alpha$ radiation was used to obtain wide angle X-ray scattering (WAXS) patterns in reflection mode of the PEEK material before and after heat treatment. A step scan interval of $2\theta = 0.1°$ was used with a 7 sec count time, and a diffracted beam graphite monochrometer. All samples were spun during exposure to average out the effects of orientation. Conditions were identical for all samples studied. Small-angle X-ray scattering (SAXS) patterns were obtained using a Statton camera geometry.

TABLE II Glass transition temperatures* of PEEK

Thermal treatment	LMW-PEEK	C-PEEK
Quenched from the melt	133	155
Unannealed†	147	170
Annealed at 230° C	147	168
266° C	147	164
302° C	138	160

*From the midpoint in the heat capacity step, 20° C min^{-1}.
†Cold crystallized at 176° C.

3. Results and discussion

3.1. Effects of long annealing time on endothermic response

DSC scans at 20° C min^{-1} are shown in Fig. 1 for LMW-PEEK. Curves 1 to 5 refer to these treatments: (1) quenched, (2) cold crystallized for 24 h at 176° C, and (3 to 5) cold crystallized as in (2) but subsequently annealed for 24 h at 230, 266 and 302° C. The sample described in (2) received a single heat treatment consisting of cold crystallization and henceforth, this will be referred to as the unannealed sample. Samples receiving the two-stage treatment (of crystallization followed by annealing) will be designated by their annealing temperature. The vertical line occurs at the location of the highest previous heat treatment. The scan of the amorphous material (1) shows a small endothermic response just above the glass transition temperature of 133° C, followed by the crystallization exotherm and a large endotherm (II) at about 340° C. The main endotherm occurs as a result of melting of crystals which crystallized during the scan and reorganized. The small endotherm at T_g may be the result of a relaxation to a state of ease, a point which will be considered later in Section 3.4.1.

The cold crystallized and annealed materials (curves 2 to 5) have the same general endothermic response

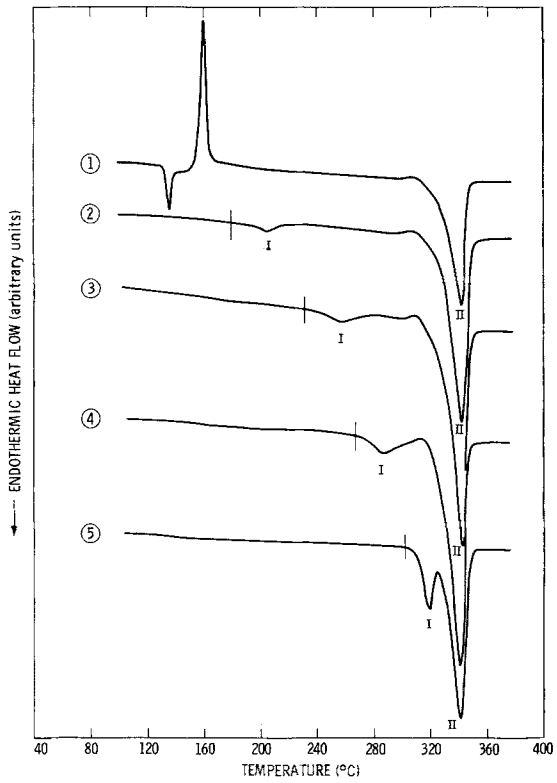

Figure 1 Endothermic response at 20° C min^{-1} of LMW-PEEK. (1) quenched, (2) cold crystallized at 176° C for 24 h, (3) to (5) as in (2) and then annealed at 230° C (3), 266° C (4), or 302° C (5).

seen in other semicrystalline polymers of low ultimate crystallinity [25–27], consisting of a small endotherm (I) just above the treatment temperature, and the high-temperature endotherm (II) whose position remains essentially constant at about 340° C. Just before the main endotherm (II) in curves 1 to 3 there appears to be a slight exothermic response at about the same temperature in all three scans.

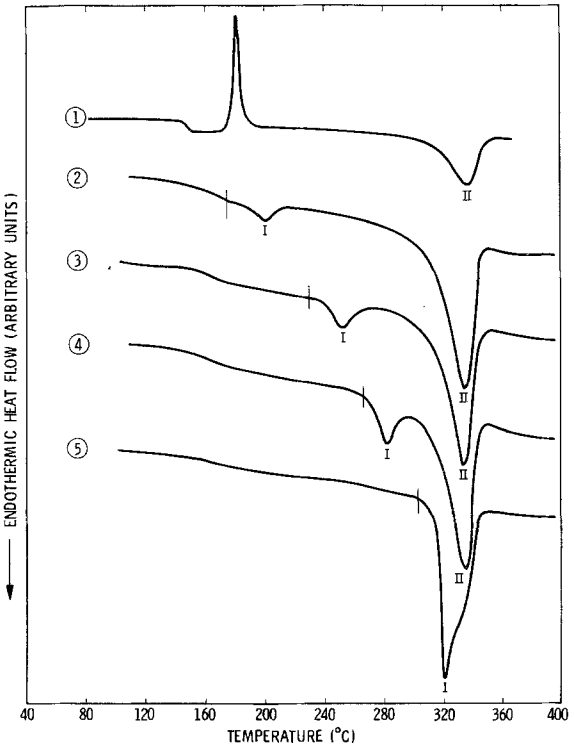

Figure 2 Endothermic response at 20° C min^{-1} of C-PEEK. Same treatment as in Fig. 1.

In Fig. 2 the endothermic response of C-PEEK is shown. Curves 1 to 5 show the same serives of treatments as for the LMW-PEEK samples just described. The quenched C-PEEK (1) shows a distinct T_g at 155° C, followed by a crystallization exotherm and a very broad main endotherm (II) at about 335° C due to reorganization of the crystals formed during the scan. The small endothermic response above T_g seen in LMW-PEEK is absent in the higher molecular weight material.

As with other semicrystalline polymers [28], crystallinity masks the appearance of the glass transition. Reduced amorphous content reduces the heat capacity step at T_g. In addition, T_g is shifted to higher temperature after crystallization. This is a reflection of the fact that molecular motion is made more difficult by crystals which act as thermoreversible cross-linking sites. In both LMW- and C-PEEK, the glass transition region is broadened, and the midpoint in the heat capacity step (which we identify with T_g) is shifted to higher temperature in the semicrystalline polymer relative to the quenched amorphous polymer. The approximate T_g values are listed in Table II. Quenched LMW- and C-PEEK glass transition temperatures are 133 and 155° C, respectively. A large increase in the midpoint of the heat capacity step occurs when the samples are cold crystallized at 176° C. After cold crystallization T_g increases about 14 to 15° C in both materials. As the treatment temperature increases, the T_g region becomes less broad and T_g shifts to a lower value. However, after crystallization and annealing, the location of T_g is still at higher temperature compared to the quenched amorphous polymer.

At the lowest annealing temperatures, the melting behaviour of C-PEEK is qualitatively similar to that of the LMW-PEEK. Again two distinct endotherms appear. The low-temperature endotherm (I) occurs just above the annealing temperature, and grows relative to (II) as the annealing temperature increases. This effect has been noted for isothermally cold crystallized PEEK [8, 16]. At the highest annealing temperature, 302°C, endotherm I dominates and endotherm II appears as a broad shoulder on the high-temperature side of the peak. In LMW-PEEK at the same temperature, endotherm I is much smaller than II.

In the endothermic response of annealed LMW-PEEK and C-PEEK (curves 3 to 5) there is no indication that the material "remembers" its previous crystallization history at 176° C. The crystals formed during the cold crystallization are not stable at higher temperature and are perfected during the very long annealing treatment. As the temperature increases above T_a, some crystals are unable to reorganize during the scan and melt just above the annealing temperature, creating endotherm I.

It is instructive to consider the interpretation of multiple endotherms which often occur when semicrystalline polymers are scanned in the DSC. For the case in which three endotherms are observed (in a polymer exhibiting a single-crystal phase) the lowest temperature endotherm usually occurs just above the original crystallization temperature. It is attributed to

the melting of small imperfect crystals which formed by secondary crystallization between existing lamellae [29]. These imperfect crystals have been referred to as subsidiary lamellae, to distinguish them from the crystals formed by primary crystallization which are called dominant lamellae. The middle endotherm in a triplet is attributed to melting of the dominant lamellae which form the majority of crystals in the sample at room temperature prior to the scan. The third and highest melting endotherm is due to the melting of a more stable recrystallized fraction that forms (reorganizes) during the scan from the crystals that created the middle endotherm.

When only a pair of well-separated endotherms is present (Fig. 1, curves 2 to 5 or Fig. 2, curves 2 to 4) there has been some debate about the nature of the endothermic response. Blundell and Osborn [8] attributed endotherm I in PEEK to the melting of all crystals present in the sample at room temperature, and endotherm II to melting of crystals formed solely during the DSC scan. Subsequently we showed [16] that after isothermal crystallization, the area under endotherm I corresponded to melting of only a very small fraction (2 to 4%) of the room-temperature population of crystals, whereas the area under endotherm II corresponded well with melting of the majority of crystals. In another case, after non-isothermal cold crystallization of PEEK [17], we found that the area under endotherm II was slightly greater than what would have been predicted from the crystallinity deduced from density or X-ray scattering. From this we concluded that, for two well-separated endotherms, endotherm II represents the melting of the majority of crystals present in the sample at room temperature, as well as those which crystallized during the scan.

Endotherms I and II may be merged, as is the case following the highest temperature treatments. Endotherm II has been shown by Cheng *et al.* [19] to arise from the melting of the dominant lamellae. After high-temperature isothermal crystallization, samples were scanned in the DSC without cooling. Endotherm II was shown to form before endotherm I at early stages of crystallization. As crystallization time was increased, endotherm I was shown to grow in after endotherm II.

Endotherm II arises from the melting of the dominant lamellae, but the temperature location of the peak is not affected by the thermal history for the wide range of annealing temperatures used here. This was found to be true also for isothermal crystallization [8, 16] as well as for the annealing treatments shown in Figs 1 and 2. Because the dominant lamellae are formed at the crystallization temperature, we might expect that their thickness would depend upon that temperature. Indeed, Blundell and Osborn [8] noted systematic increases in the long period and in Section 3.4.3 we show that similar changes in the long period occur after the annealing treatments just described. If the dominant lamellae produce the room temperature SAXS patterns, and increase in thickness with increasing treatment temperature, we must consider why their endothermic response is invariant with treatment temperatures. Several explanations may be suggested. First, the relationship between melting point and lamellar thickness, derived for melt crystallization at low degree of undercooling, may be an inadequate representation for crystallization from the rubbery amorphous state at very high degree of undercooling. Second, the dominant lamellae may be metastable, such that when the temperature increases during the DSC scan they thicken into the regions previously occupied by the subsidiary lamellae, without melting. These reorganized crystals may then melt at about the same temperature regardless of original treatment temperature. We shall tentatively adopt the second viewpoint, and will refer to endotherm II as a reorganization endotherm resulting from melting of the dominant lamellae.

In Table III the peak melting temperatures for endotherms I and II are listed along with the heats of fusion for both LMW- and C-PEEK. Peak temperatures were chosen because of the breadth of the endothermic response. The first four rows in the table refer to samples described in Figs 1 and 2. The last two rows pertain to samples to be described in Section 3.2. At all treatment temperatures, except 302° C, the melting points of LMW-PEEK are greater than those of C-PEEK. The peak temperature of endotherm II is from 6 to 9° C higher in LMW-PEEK than in C-PEEK. Heats of fusion range from 41 to 53 J g^{-1} in C-PEEK and from 64 to 73 J g^{-1} in LMW-PEEK where dual endotherms merged (for example in Fig. 1, curve 5), the area listed in Table II is the total area under endotherms (I + II). Where the dual endotherms were widely separated, only the area under endotherm II is listed.

In some cases, a single endotherm was observed in

TABLE III Peak melting temperatures* and heats of fusion for heat treated LMW- and C-PEEK

Thermal treatment	LMW-PEEK			C-PEEK		
	T_m(l) (° C)	T_m(u) (° C)	H_f (J g^{-1})	T_m(l) (° C)	T_m(u) (° C)	H_f (J g^{-1})
Unannealed†	204	343	68	201	334	41
T_a = 230° C	259	344	66	253	335	38
266° C	289	341	64	282	335	39
302° C	321	342	73	321	321	50
T_a = 302° C‡	323	339	58	331	331	50
310° C‡	334	343	64	338	338	53

*Lower melting point, T_m(l), and upper melting point, T_m(u), in samples having dual endothermic response (I and II). Heating rate 20° C min^{-1} for all table entries.
†Cold crystallized at 176° C, 24 h.
‡Annealed without prior cold crystallization at 176° C.

C-PEEK and in LMW-PEEK. The appearance of a single endotherm will depend upon the thermal history of the sample [31, 32]. For example, in the case of annealing of C-PEEK at 302° C, the single endotherm (I) represents the melting of the preformed crystal structure (dominant lamellae) that existed in the sample at room temperature. However, for both C-PEEK and LMW-PEEK, the single endotherm seen in a scan of originally amorphous material has a different origin. In this case, the single endotherm is due to the complete transformation of material that had crystallized and reorganized during the scan, and hence, does not reflect the state of this material immediately after crystallization. In LMW-PEEK and in C-PEEK, endotherm I or II may be absent in a given DSC scan depending upon the relative stability of the material. When both I and II are present, the low-temperature endotherm may represent the melting of only a very small portion of the crystals. The remaining material may continue to thicken without melting during the scan and contribute to endotherm II which may then be independent of original treatment temperature. In this case, neither endotherm will have a peak temperature that represents the true melting point of the preformed crystal structure at room temperature.

3.2. Effects of scanning rate

From the previous discussion we may expect the DSC scanning rate to affect the endothermic response. Variation of the scanning rate changes the residence time at a given temperature and will therefore affect the reorganization during the DSC scan [24–26]. Effects of residence time on the sequence of formation of endotherms I and II have been considered [19] for isothermal melt crystallization. It was shown that, for $T_c = 310°C$, the upper endotherm (II) develops before the lower (I), and not as a result of complete reorganization of endother I into endotherm II. It is of interest to compare the behaviour of our annealed PEEK materials, heated from the rubbery amorphous state to high temperature, with PEEK isothermally crystallized from the melt [19] in the same temperature range. For both molecular weights, slower heating rates should allow the least perfect material to thicken to a higher melting form as the temperature increases above the nominal melting point, contributing to endotherm II. Faster heating rates should minimize reorganization and cause superheating. These effects were observed in both LMW- and C-PEEK samples annealed (without prior cold crystallization) at 302 and 319° C for 24 h. Results are shown in Fig. 3 (LMW-PEEK) and 4 (C-PEEK) for several heating rates. For comparison with the samples described in Section 3.1, the endotherm areas and melting points at 20° C min^{-1} of the present samples are listed in the last two rows of Table III.

Dual endotherms are observed for LMW-PEEK, Fig. 3a, after 302° C annealing for all scanning rates from 5 to 40° C min^{-1}. Endotherm I grows relative to endotherm II, and the peak temperature of endotherm I increases with increasing scan rate. The peak temperature of endotherm II decreases with rate until the fastest rate, where its increase is probably due to superheating. For this range of scan rates, LMW-PEEK is not stable against reorganization when annealed at 302° C. That is, the later-forming subsidiary lamellae melting to produce endotherm I may reorganize and contribute to endotherm II at the lower scan rates. This could occur in one of two ways: either the

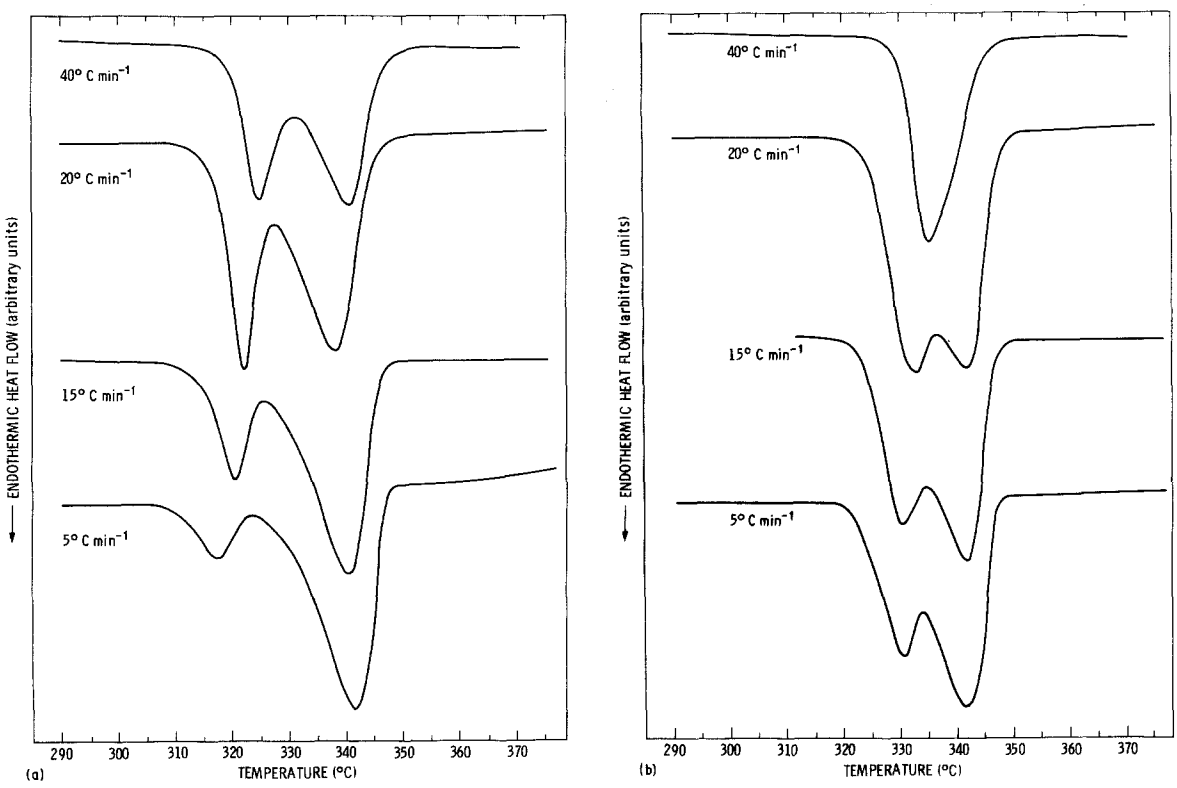

Figure 3 Endothermic response of LMW-PEEK at the indicated rates. (a) Annealed at 302° C for 24 h, (b) annealed at 319° C for 24 h.

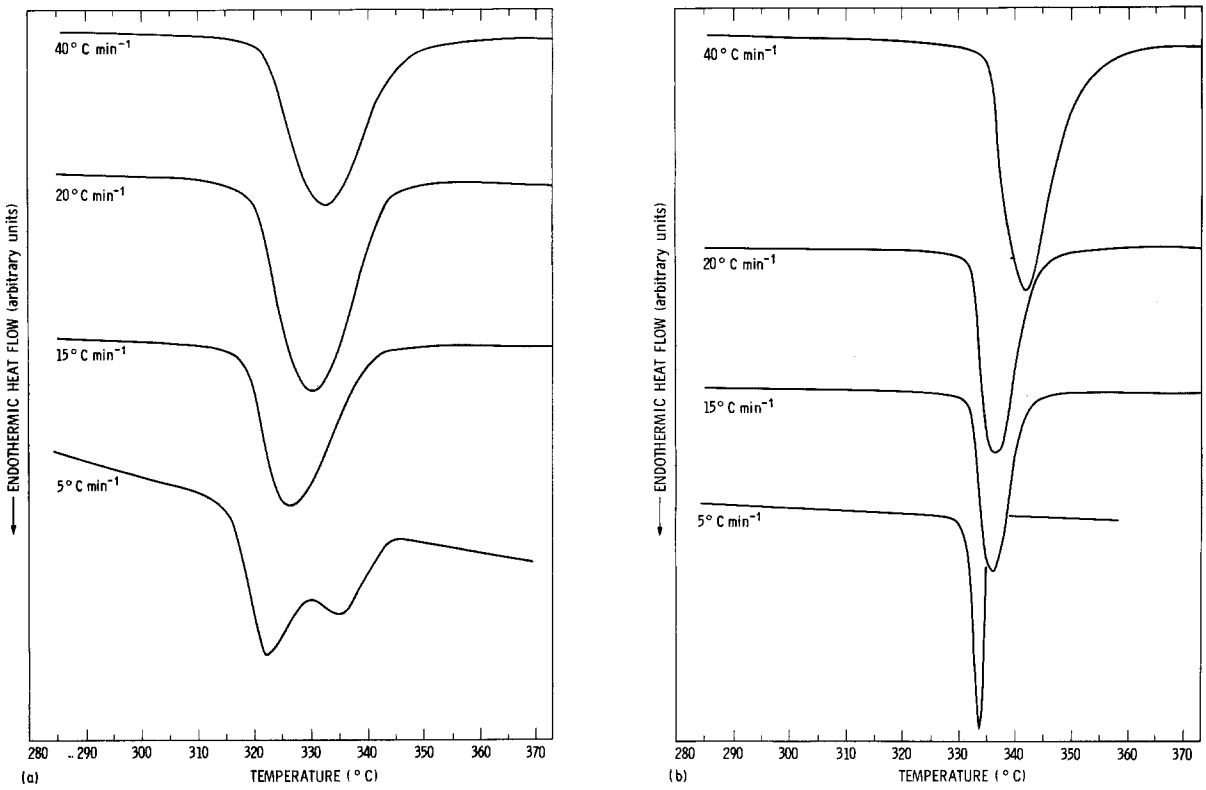

Figure 4 Endothermic response of C-PEEK at the indicated rates. (a) and (b) as in Fig. 3.

subsidiary lamellae could melt and recrystallize into higher melting, thicker lamellae, or they could melt and provide available amorphous chains for further growth of the dominant lamellae. The first process of recrystallization may be less favourable due to the slow rate of crystallization at these temperatures. When the annealing temperature is increased to 319° C, Fig. 3b, endotherm II diminishes relative to endotherm I, and at 40° C min^{-1} the two cannot be resolved. Once again the temperature of endotherm I increases with scan rate, while the temperature of endotherm II decreases slightly. After annealing at 319° C, the area under endotherm I is much greater relative to endotherm II than at 302° C. The higher temperature annealing at 319° C results in more stable subsidiary lamellae.

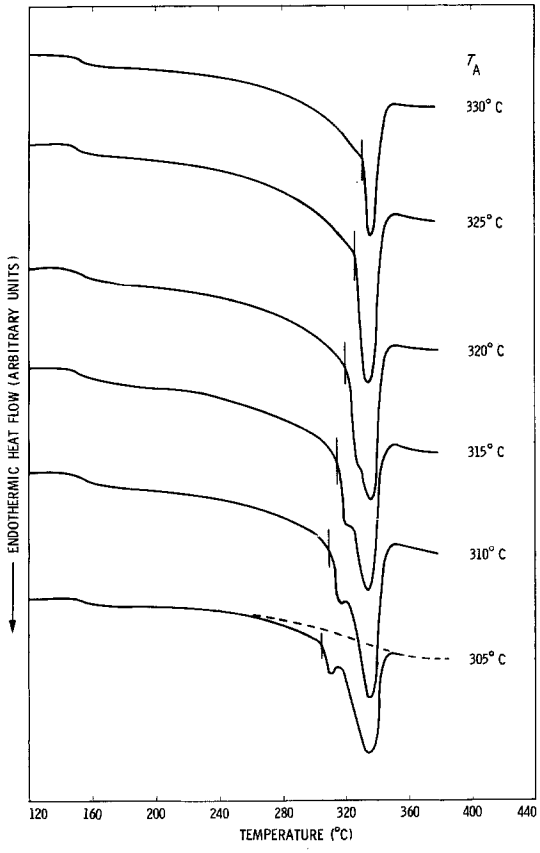

Figure 5 Endothermic response of LMW-PEEK rapidly annealed at the indicated temperatures. $\dot{T} = 20° C min^{-1}$.

Results are shown in Fig. 4 for the C-PEEK material. Annealing at 319° C (Fig. 4b) produces a single endotherm for all rates studied, and for rates of 15° C min^{-1} or greater when the annealing temperature is 302° C (Fig. 4a). Dual endothermic response occurred only for 302° C annealing at the slowest heating rate. Endotherm II present at 302° C, 5° C min^{-1}, merges with endotherm I as the rate increases, and the peak temperature of the remaining endotherm increases as a result of superheating. The remaining endotherm is broader after 302° C annealing which indicates that there is a broader distribution of crystallite sizes. After very high temperature annealing, the single endotherm of C-PEEK material most nearly represents the melting point of the majority of crystals present in the sample at room temperature. This treatment temperature is very close to that used by Cheng *et al.* [19] for isothermal melt crystallization. In Table III of [19], effects of scan rates from 0.31 to 10 K min^{-1} are shown. Dual endothermic response was reported, with the area under the lower peak (I) decreasing with decreasing rate, and the area under the higher peak (II) increasing. In contrast, our results indicate that annealing at 319° C by heating from the rubbery state creates a different morphology in which the material can be characterized by a single broad endotherm, for the rates studied.

3.3. Effects of short annealing time

Effects of very short annealing times were studied for LMW- and C-PEEK annealed at high temperatures near the nominal melting point. Endothermic response is shown in Figs 5 (LMW-PEEK) and 6 (C-PEEK) for quick annealing treatments at the temperatures indicated by the vertical markers. All DSC scans were obtained at 20° C min^{-1}. Dual endotherms are seen in LMW-PEEK at the lowest annealing temperatures, and as T_a increases, endotherm I diminishes until T_a = 320° C. At higher T_a, endotherm I is barely evident as a should on the low-temperature side of endotherm II. This is in contrast to the behaviour shown in Fig. 3b after a very long annealing time at 319° C, in which case endotherm II becomes merged with endotherm I at the highest scanning rate. After long annealing, the crystal population has achieved a level of perfection such that reducing the residence time at high temperature (increasing scan rate) serves to prevent the material from reorganizing. After brief annealing, however, the crystal population may be very imperfect and subject to rapid reorganization. In fact, at the highest annealing temperatures, the LMW-PEEK may still remain in the molten state with a large fraction of crystals forming only during cooling. This is supported by the endothermic departure from the baseline at temperatures just below T_a, and absence of endotherm I at T_a > 320° C.

Similar conclusions can be made about the behaviour of C-PEEK after brief annealing in the same temperature range, shown in Fig. 6. The empty cell baseline curvature is indicated by the dashed line in the lowest curve. In all scans there is a departure from the baseline below T_a, caused by the melting of crystals which had remained molten at T_a, but crystallized during cooling. Dual endotherms can be seen distinctly in the samples annealed at the lowest annealing temperatures, from 305 to 320° C. The low-temperature endothermic responses represent the melting of the crystals formed during the annealing stage. The remaining samples, which were annealed much closer to the nominal 335° C melting point, show only a poorly resolved single endotherm. In Table IV, the peak temperatures and heats of fusion are listed for the rapidly annealed samples.

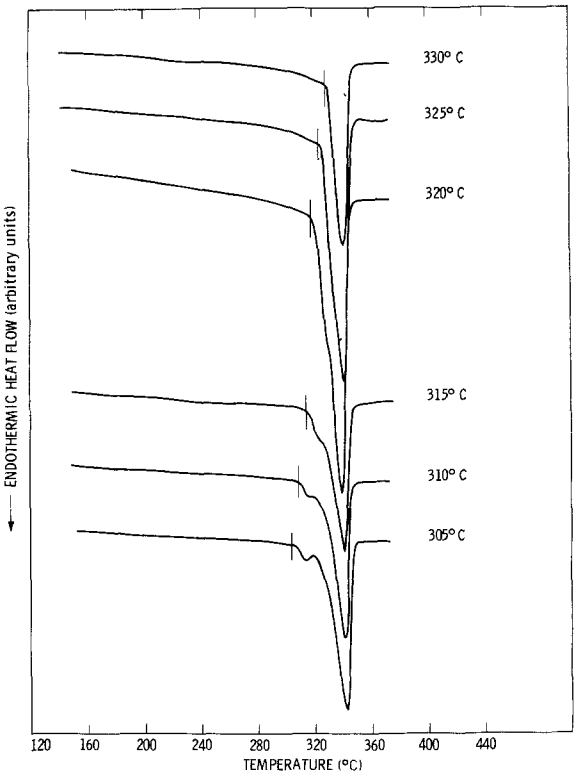

Figure 6 Endothermic response of C-PEEK rapidly annealed at the indicated temperatures. $\dot{T}$ = 20° C min^{-1}.

The variation of melting temperature with annealing temperature is shown in Fig. 7 for all annealing treatments. Where dual endotherms occurred, only the lower endotherm I is plotted. For comparison, several sets of data for isothermal crystallization are also shown. The isothermal crystallization data are from Blundell and Osborn [8] (●), Cheng *et al.* [19] (◆), and from our own laboratory [33] (■). For our data, a vertical marker has been used to show the spread in melting temperatures as a function of DSC scanning rate. The upper limit indicates the peak melting temperature at 50° C min^{-1} while the lower limit indicates T_m for 5° C min^{-1}. The data point locates T_m at a rate of 20° C min^{-1}. All the melting point data fall within a narrow band having a spread of about 15° C.

For isothermal melt crystallization at low undercooling, a linear relation between T_m and the crystallization temperature, T_c, has been predicted by the kinetic theory of polymer crystallization [34] and is usually written

$$T_m = T_m(0)[(g - 1)/g] + T_c/g \qquad (1)$$

where $T_m(0)$ is the equilibrium melting point and g is a ratio of lengths of lamellae formed at T_c to the length of the critical nucleus at T_c. Several assumptions are implicit in the derivation of Equation 1, namely (i) the degree of undercooling must be low, and (ii) terms that relate to the side surface free energy must be small relative to terms in the fold surface free energy. The infinite crystal melting point, $T_m(0)$, is found from the intersection of the line described by the data with that defined by $T_m = T_c$. When the isothermal crystallization data (● [8], ◆ [19], and □ [33]) are extrapolated to the intersection with $T_m = T_c$ the infinite crystal melting point is much larger than 395° C. It is likely that for isothermal cold crystallization from the rubbery amorphous state, neither assumption (i) nor (ii) is valid.

3.4. Effects of annealing on properties

3.4.1. Microstructural changes induced by annealing

Improvement in crystalline microstructure after annealing is indicated in Figs 8a (LMW-PEEK) and b (C-PEEK) from WAXS patterns of representative annealed samples. The dashed line in the lowest curve is the scattering pattern from the quenched sample. In the case of LMW-PEEK, the intensity from the quenched sample is coincident with that of the cold crystallized sample below 17°. There are two distinct features in the WAXS patterns that change with annealing treatment: the sharp crystalline reflections,

TABLE IV Peak melting temperatures* and heats of fusion for rapidly annealed LMW- and C-PEEK

Annealing temperature (°C)	LMW-PEEK			C-PEEK		
	T_m(l) (°C)	T_m(u) (°C)	H_f (J g^{-1})	T_m(l) (°C)	T_m(u) (°C)	H_f (J g^{-1})
305	314	342	62	312	335	33
310	318	342	61	317	335	37
315	323	341	66	321	335	39
320	328	340	65	326	335	37
330	342	342	68	337	337	43

*Lower melting point, T_m(l), and upper melting point, T_m(u) in samples having dual endothermic response.

reported previously [8], and a broad maximum at 14°. The existence of this broad scattering at 14° has been reported by our group for C-PEEK samples used in mechanical properties tests [35], and in commercially available APC-2 PEEK composites [6]. With regard to the crystalline reflections, the broadness of the peaks precludes a quantitative determination of the crystallite size but, qualitatively we can say that samples annealed at higher annealing temperatures have more perfect crystals. In both LMW-PEEK and C-PEEK, the crystalline reflections become narrower (smaller full-width at half-maximum) and are better resolved from the amorphous scatter as the annealing temperature increases. Recently, Wakelyn [36] has shown that annealing results in increases of the crystallographic densities by as much as 3%.

The broad maximum at 14° is present in both quenched and annealed LMW-PEEK and, as the annealing temperature increases, this peak intensity greatly increases. At the highest T_a, the intensity at 14° equals that of the crystalline (1 1 0) reflection. In C-PEEK, only the annealed samples show the 14° scattering peak, and it is less distinct in the higher molecular weight material. If the samples shown in Fig. 8 (curve 4 solid line) are heated above their glass transitions (to 145° C for LMW-PEEK, or to 180° C for C-PEEK) and then slowly cooled, the intensity at 14° is redistributed. This is shown in Fig. 8, curve 4 broken lines. Different samples were used to produce the two curves and no attempt was made to normalize the intensities for differences in scattering volume. Nonetheless, in both materials the large feature at 14° has been eliminated by heating above T_g and slowly cooling. When quenched LMW-PEEK was heated above T_g and then scanned in the DSC, the small endothermic peak (seen just above T_g in Fig. 1, curve 1) was eliminated, evidence of a relaxation to a more stable configuration.

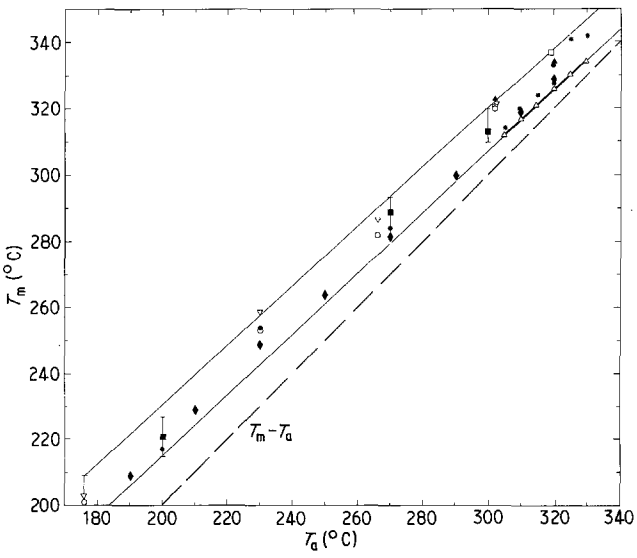

Figure 7 Melting point, $T_m(l)$, of endotherm I plotted against treatment temperature, T_a: Cold crystallization at 176° C followed by annealing, (▽) LMW-PEEK (○) C-PEEK. Annealing without prior cold crystallization at 176° C, (△) LMW-PEEK; (□) C-PEEK. Rapid annealing, (*) LMW-PEEK; (△) C-PEEK. Isothermal crystallization of C-PEEK, (●) Blundell and Osborn [8]; (◆) Cheng *et al.* [19]; (■) Cebe [33]. See text for explanation of vertical markers.

The redistribution of scattering intensity involves first, an increase in the baseline level of scattering at all scattering angles, and second, a shift in intensity from the 14° position to higher angles. This shift is seen to increase the scattering in the region from 25° to 27°, a region normally associated with purely amorphous scattering (note the coincidence of amorphous and semi-crystalline scatter in this region, as shown in curves 1). Thus, a large effect is seen in the amorphous scattering profile after hearing above T_g and slowly cooling. In addition, for LMW-PEEK, the peak positions of the crystal reflections are also affected by the slow cooling treatment. The *d*-spacings are reduced after treatment for all four reflections. The same thing was observed in C-PEEK to a lesser extent. This suggests that the disorder may be associated with the crystal–amorphous interface region, and may possibly be the result of residual stresses induced during fast cooling.

3.4.2. Cross-linking after annealing treatments

Samples were tested for possible chemical cross-linking after the annealing treatments described in Sections 3.1. and 3.2. These treatments involved annealing temperatures in the range from 230 to 302° C, for a time of 24 h. After the annealing, samples of LMW-PEEK and C-PEEK were heated in α-chloronaphthalene under constant flow or argon to 238° C. At this temperature all samples dissolved in a few minutes, indicating that no cross-linking resulted from the annealing treatments. Cross-linking was observed to occur, however, when the annealing temperature was increased to 319° C. Samples of LMW-PEEK and C-PEEK swelled in α-chloronaphthalene as the temperature was increased to 260° C. After boiling for 1 h the C-PEEK was cooled, washed in methylethylketone, and the weight loss recorded. The LMW-PEEK material fell into string-like pieces and could not be recovered for weighing. The weight

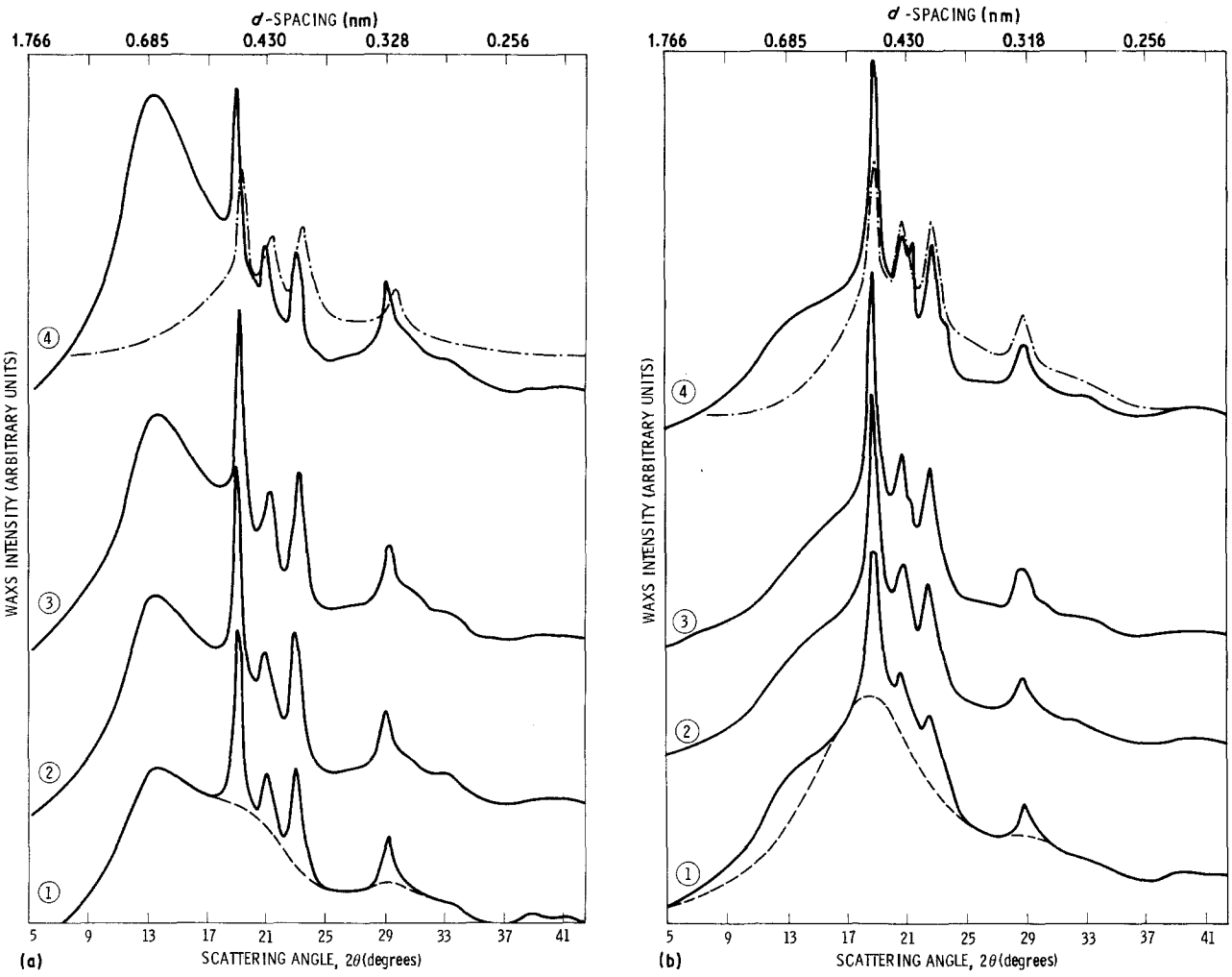

Figure 8 WAXS intensity plotted against scattering angle for (a) LMW-PEEK and (b) C-PEEK. (1) cold crystallized at 176° C (——), quenched amorphous (– – –); (2 to 4) cold crystallized at 176° C and then annealed at 230° C (2), 266° C (3), or 302° C (4); quickly cooled after annealing (——), heated above T_g and slowly cooled (–·–·–·–).

loss of the C-PEEK depended upon the crystallization history prior to annealing. When the material was cold crystallized at 176° C for 24 h, then annealed 24 h at 319° C, the weight loss was 25%. For C-PEEK annealed without prior cold crystallization the weight loss was 60%. The cold crystallized sample was more heavily cross-linked (smaller soluble fraction).

As crystallinity may impede the action of the solvent we performed another test to verify that chemical cross-linking indeed had taken place. A C-PEEK film annealed at 319° C after prior cold crystallization was heated to the melting point and quenched to form a clear amorphous material. This film was treated in α-chloronaphthalene, as above, and after boiling for 1 h it had swelled but did not dissolve. The measured weight loss of this film was 28%, about the same as its semicrystalline counterpart. From this we conclude that it is possible to cross-link C-PEEK using certain thermal treatments. When the annealing temperature is high, 319° C or greater, annealing for 24 h will cause chemical cross-linking. However, annealing temperatures of 302° C or lower for the same time did not result in cross-linking. Because the annealing treatments were performed in the presence of oxygen, it seems likely that the cross-linking could be an effect of high-temperature oxidation, a point we are investigating further.

3.4.3. *Density, crystallinity, and lamellar thickness of annealed PEEK*

Density measurements were made to ascertain the degree of crystallinity in C-PEEK. Poor sample quality prevented similar measurements in LMW-PEEK. Measurements were made on material immediately after fast cooling and again after the material had been heated above the glass transition and slowly cooled. The density results are listed in the first two columns of Table V. Mass fraction crystallinity was computed for the slowly cooled polymer on the assumption that this material could be adequately represented as a two-phase system of crystalline and amorphous components. The slowly cooled material is more dense in all cases, which is in agreement with the general shift in WAXS intensity to smaller d-spacing after slower cooling through T_g. Mass fraction crystallinity deduced from density increases with the annealing temperature, from 0.26 to 0.40.

The area under the DSC endotherm was used as another measure of degree of crystallinity, and these results are also shown in Table V. Degree of crystallinity, X_c, was computed from $X_c = H_F(\text{meas})/H_F$, where $H_F(\text{meas})$ is the apparent heat of fusion, and H_F is the heat of fusion of perfectly crystalline PEEK. Results of DSC peak area measurements are complicated by the tendency for reorganization during

TABLE V Microstructural parameters for annealed C-PEEK

T_a (°C)	Density ($g\,cm^{-3}$)		X_c(m)* (%)	H_F ($J\,g^{-1}$)	X_c(m)† (%)	L (nm)	l (nm)
	Quickly cooled	Slowly cooled					
Unannealed	1.2909	1.2945	26	40.7	31	9.8	2.5
230	1.2964	1.3002	30	38.0	29	11.0	3.3
266	1.3002	1.3039	34	39.5	30	13.4	4.6
302	1.3053	1.3083	38	49.7	38	15.5	5.9
302‡	1.3064	1.3095	39	49.7	38	15.4	6.0
319‡	1.3075	1.3104	40	53.3	41	15.4	6.2

*Mass fraction deduced from density.
†Mass fraction crystallinity deduced from heat of fusion.
‡Heated directly to T_a without cold crystallization at 176° C.

the scan. Area under the sum I + II was used to determine X_c when the dual endotherms were merged; only endotherm II was used when they were widely separated.

Best agreement was obtained between the density and DSC determinations of mass fraction crystallinity when there was overlop of low- and high-temperature endotherms. This situation occurred only at the highest annealing temperatures. One explanation for this may be that the density measurements are made at room temperature, and are characteristic of the room temperature state of the material. In the DSC results material that was annealed at high temperature is now thermally very stable and thus will have a peak area that is more representative of the actual crystallinity of the room-temperature material.

Small-angle X-ray scattering was used to determine the long period, L, of the annealed C-PEEK samples. These values are listed in Table V along with the lamellar thickness, l, which was calculated from $l = (X_c)(L)$. The volume crystallinity, X_c, is that determined from the density of the ordered state of the material. The long period increases from 9.8 nm in the cold crystallized film to 15.4 nm in the samples annealed nearer to the melting point. The long periods are larger than previously reported [8] due to the much longer annealing times used in the current study.

4. Conclusions

We have examined the effects of annealing after cold crystallization for two PEEK materials of different molecular weight. Cold crystallization and annealing resulted in materials with substantially higher glass transition temperatures, compared to the amorphous state. Long annealing resulted in increased density, greater crystal perfection, and increased long period.

For both high- and low-molecular weight PEEK, the endothermic response is a complex function of crystallization history, annealing time and temperature, and DSC scanning rate. As in other thermoplastics that can be cold crystallized from the rubbery amorphous state, PEEK melting behaviour may consist of several endotherms. When the annealing temperature is below 300° C, a pair of widely separated endotherms is observed in both high- and low-molecular weight PEEK. The lower temperature endotherm (I) represents the melting of a small population of imperfect crystals (subsidiary lamellae), while the higher temperature endotherm (II) represents the melting of the majority population of crystals in the sample at room temperature as well as those which crystallize during the scan. That the peak position of (II) is independent of treatment temperature is attributed to thickening of the dominant lamellae during the scan. In some instances, a single endotherm was observed. Quenched amorphous material that crystallizes during the scan displays a single reorganization endotherm because the crystals formed non-isothermally at low temperatures are very unstable and reorganize continuously to higher melting forms. Long annealing treatments at high temperatures (> 300° C) resulted in a single broad endotherm for high-molecular weight PEEK at nearly all scanning rates. It is likely that endotherms I and II become merged while that of endotherm II decreases. For lower molecular weight PEEK, a higher scanning rate of $40°\,C\,min^{-1}$ was required before the two endotherms merged. This implies that the lower melting subsidiary lamellae are more stable against superheating, and the higher melting dominant lamellae are more stable against reorganization, in the lower molecular weight material.

Acknowledgements

The author wishes to thank Professor D. C. Bassett for helpful discussions. This research was performed by the Jet Propulsion Laboratory, California Institute of Technology, under contract with the National Aeronautics and Space Administration.

References

1. J. PETERMAN and J. M. SCHULTZ, *J. Mater. Sci.* **13** (1978) 2188.
2. D. SHINOZAKI and G. W. GROVES, *ibid.* **11** (1976) 2356.
3. G. GROENINCKX and H. REYNAERS, *J. Polym. Sci. Polym. Phys. Edn* **18** (1980) 1325.
4. M. PARVIN, *J. Mater. Sci.* **16** (1981) 1796.
5. J. A. ZURINENDI, F. BIDDLESTONE, J. N. HAY and R. N. HAWARD, *ibid.* **17** (1982) 199.
6. P. CEBE, S. Y. CHUNG and A. GUPTA, ACS Symposium on Composites, Anaheim, California, September (1986).
7. T. KUNUGI, A. MIZUSHIMA and T. HAYAKAWA, *Polym. Commun.* **27** (6) (1986) 175.
8. D. J. BLUNDELL and B. N. OSBORN, *Polymer* **24** (1983) 953.
9. A. J. LOVINGER and D. D. DAVIS, *J. Appl. Phys.* **58** (1985) 2843.
10. *Idem, Polym. Commun.* **26**(11) (1985) 322.
11. S. KUMAR, D. P. ANDERSON and W. W. ADAMS, *Polymer* **27** (1986) 329.

12. J. N. HAY, D. J. KEMMISH, J. I. LANGFORD and A. I. M. RAE, *Polym. Commun.* **26**(6) (1984) 175.
13. P. C. DAWSON and D. J. BLUNDELL, *Polym. Reports* **21**(5) (198) 577.
14. D. R. RUEDA, F. ANIA, A. RICHARDSON, I. M. WARD and F. J. BALTA CALLEJA, *Polym. Commun.* **24**(9) (1983) 258.
15. D. J. KEMMISH and J. N. HAY, *Polymer* **26** (1985) 905.
16. P. CEBE and S.-D. HONG, *ibid.* **27** (1986) 1183.
17. P. CEBE, *Polym. Preprints* **27** (1986) 449.
18. A. J. LOVINGER and D. D. DAVIS, *Macromol.* **19** (1986) 1861.
19. S. Z. D. CHENG, M. Y. CAO and B. WUNDERLICH, *ibid.* **19** (1986) 1868.
20. H. X. NGUYEN and H. ISHIDA, *Polymer* **27** (1986) 1400.
21. *Idem, J. Polym. Sci. Polym. Phys. Edn* **24** (1986) 1079.
22. T. E. ATTWOOD, P. C. DAWSON, J. L. FREEMAN, L. R. J. HOY, J. B. ROSE and P. A. STANILAND, *Polymer* **22** (1981) 1096.
23. J. DEVAUX, D. DELIMAY, D. DAOUST, R. LEGRAS, J. P. MERCIER, C. STAZIEL and E. NIELD, *ibid.* **26** (1985) 1994.
24. P. J. FLORY, "Principles of Polymer Chemistry" (Cornell University Press, Ithaca, New York, 1953).
25. N. OVERBERGH, H. BERGHMANS and G. SMETS, *J. Polym. Sci. C* **38** (1972) 237.
26. P. J. HOLDSWORTH and A. TURNER-JONES, *Polymer* **12** (1971) 195.
27. G. GROENINCKX, H. REYNAERS, H. BERGHMANS and G. SMETS, *J. Polym. Sci. Polym. Phys. Edn* **18** (1980) 1311.
28. R. F. BOYER, *J. Polym. Sci. Symp.* **50** (1975) 189.
29. D. C. BASSETT, "Principles of Polymer Morphology" (Cambridge University Press, Cambridge, 1981).
30. E. HELLMUTH and B. WUNDERLICH, *J. Appl. Phys.* **36** (1965) 3039.
31. M. JAFFEE and B. WUNDERLICH, *Kolloid Z. Z. Polym.* **216** (1966) 203.
32. B. WUNDERLICH, in "Macromolecular Physics", Vol. 2 (Academic, New York, 1976).
33. P. CEBE, unpublished results.
34. J. D. HOFFMAN, G. T. DAVIS and J. I. LAURITZEN, in "Treatise on Solid State Chemistry" (Plenum, New York, 1976) p. 497.
35. P. CEBE, S. Y. CHUNG and S.-D. HONG, *J. Appl. Polym. Sci.* **33** (1987) 487.
36. N. T. WAKELYN, *J. Polym. Sci. Polym. Lett.* **25** (1987) 25.

Received 3 March
and accepted 15 July 1987